Kinetic Modeling of Fermentative Production of 1, 3-Propanediol by *Klebsiella pneumoniae* HR526 with Consideration of Multiple Product Inhibitions

Lu He · Xuebing Zhao · Keke Cheng · Yan Sun · Dehua Liu

Abstract During the fermentative production of 1, 3-propanediol (1,3-PD), the multiple product inhibitions cannot be negligible to accurately describe the kinetics of fermentation process. A kinetic model for fermentative production of 1,3-PD by *Klebsiella pneumoniae* HR526 with glycerol as carbon source under aerobic condition was proposed. The inhibitions of multiple products including 1,3-PD, 2, 3-butanediol (2,3-BD), acetate, and succinate were considered in the model. It was found that 1,3-PD, 2,3-BD, and acetate showed strong inhibitions to cell growth depending on their concentrations. The kinetic model was relatively accurate to predict the experimental data of batch, fed-batch, and continuous fermentations. The model thus can serve as a tool for further controlling and optimizing the fermentation process.

Keywords 1, 3-propanediol · Kinetic modeling · Fermentation · Product inhibition · *Klebsiella pneumoniae*

Nomenclature

X	Cell biomass concentration ($g \cdot L^{-1}$)
P	1,3-PD concentration ($g \cdot L^{-1}$)
P_B	2,3-BD concentration ($g \cdot L^{-1}$)
P_A	Acetate concentration ($g \cdot L^{-1}$)
P_S	Succinate concentration ($g \cdot L^{-1}$)
S	Glycerol concentration ($g \cdot L^{-1}$)
μ_m	Maximum specific growth rate (h^{-1})
K_S	Saturation constant for cell growth rate ($g \cdot L^{-1}$)
α	Kinetic constant for 1,3-PD formation from cell growth ($g \cdot g^{-1}$)

L. He · X. Zhao (✉) · Y. Sun · D. Liu (✉)
Institute of Applied Chemistry, Department of Chemical Engineering, Tsinghua University,
Beijing 100084, China
e-mail: zhaoxb@mail.tsinghua.edu.cn
e-mail: dhliu@tsinghua.edu.cn

K. Cheng
Institute of Nuclear and New Energy Technology, Tsinghua University, Beijing 100084, China

β Kinetic constant for 1,3-PD formation from biomass (h^{-1})

α_B Kinetic constant for 2,3-BD formation from cell growth ($g \cdot g^{-1}$)

β_B Kinetic constant for 2,3-BD formation from biomass (h^{-1})

α_A Kinetic constant for acetate formation from cell growth ($g \cdot g^{-1}$)

β_A Kinetic constant for acetate formation from biomass (h^{-1})

α_S Kinetic constant for succinate formation from cell growth ($g \cdot g^{-1}$)

β_S Kinetic constant for succinate formation from biomass (h^{-1})

$Y_{X/S}$ Yield coefficient of biomass on glycerol ($g \cdot g^{-1}$)

$Y_{P/S}$ Yield coefficient of 1,3-PD on glycerol ($g \cdot g^{-1}$)

$Y_{PB/S}$ Yield coefficient of 2,3-BD on glycerol ($g \cdot g^{-1}$)

$Y_{PA/S}$ Yield coefficient of acetate on glycerol ($g \cdot g^{-1}$)

$Y_{PS/S}$ Yield coefficient of succinate on glycerol ($g \cdot g^{-1}$)

n Kinetic constant for glycerol consumption on cell metabolism (h^{-1})

C_P^* Critical inhibition concentration for 1,3-PD of maximum specific growth rate ($g \cdot L^{-1}$)

C_B^* Critical inhibition concentration for 2,3-BD of maximum specific growth rate ($g \cdot L^{-1}$)

C_A^* Critical inhibition concentration for acetate of maximum specific growth rate ($g \cdot L^{-1}$)

P^* Critical feedback inhibition concentration of 1,3-PD for 1,3-PD formation ($g \cdot L^{-1}$)

P_B^* Critical feedback inhibition concentration of 2,3-BD for 2,3-BD formation ($g \cdot L^{-1}$)

P_A^* Critical feedback inhibition concentration of acetate for acetate formation ($g \cdot L^{-1}$)

P_S^* Critical feedback inhibition concentration of succinate for succinate formation ($g \cdot L^{-1}$)

Introduction

1, 3-propanediol (1,3-PD) is an important chemical widely used in ink, coating, medicine, lubricant, antifreeze, and other industries [1]. One of the major application of 1,3-PD refers to the synthesis of polytrimethylene terephthalate (PTT), which is a novel polyester material with extraordinary properties and excellent performance [2]. Compared with other traditional polyester materials such as PET and PBT, PTT is superior in elastic recovery, stain resistance, good dyeing properties, anti-static electricity, and especially biodegradability. Therefore, PTT has attracted more and more attention in a variety of areas such as textile, plastic, and carpet [3]. As a monomer for synthesizing PTT, 1,3-PD has a considerable market prospect. 1,3-PD can be produced by either chemical synthesis or microbial fermentation. Compared to chemical synthesis, microbial fermentation has some advantages such as good selectivity, high conversion rate, mild reaction conditions, simple operations, low energy cost, and less pollution. Besides, during microbial fermentation renewable resources can be used as raw materials, which shows a green sustainability for an industrial production of 1,3-PD [4–8]. A typical biorefinery platform has been developed in our previous work, by which various oil feedstocks can be converted to biodiesel with the by-product glycerol being converted to 1,3-PD by bacterial fermentation [9].

Klebsiella pneumoniae is a promising bacteria producing 1,3-PD with high productivity and yield, and its metabolic mechanism has been intensively studied in literatures [10–14]. However, most reported works of 1,3-PD fermentation by *K. pneumoniae* are focused on the optimizations of culture medium and processes [15–18], and most of the studies on kinetic modeling of 1,3-PD production are for the processes under anaerobic condition [19–21]. In our previous work we isolated a *K. pneumoniae* strain (*K. pneumoniae* HR526) which showed an excellent production capacity under aerobic condition and achieved a 1,3-PD

concentration of 91.47 gL^{-1}, a molar conversion rate of 0.52 $molmol^{-1}$ and a productivity of 3.13 $gL^{-1}h^{-1}$ after a 30-h fed-batch fermentation [22]. This strain has also been successfully employed for the pilot-scale and industrial production of 1,3-PD [23]. The metabolic flux and key enzyme activities of 1,3-PD synthesis also have been analyzed [13, 22]. However, the accumulations of multiple products can exert strong inhibitions to cell growth and 1,3-PD synthesis, which makes it difficult to analyze and control the process. Zeng et al. proposed a kinetic model to describe substrate and ATP consumption rates of microbial growth under substrate-sufficient conditions [21]. However, Xiu et al. found that the model should be modified when initial glycerol concentration was consumed at a high rate [24]. They further improved the kinetic model in order to describe substrate consumption and products formations in a large range of feed glycerol concentration, and determined the kinetic constants by continuous fermentation results, and the model could give a good description of the steady-state continuous fermentation and predict the occurrence of multiplicity. However, the model fails to satisfactorily describe the fermentation process in our experiments with deviation of higher than 40 %. It is probably because that the model parameters were determined by anaerobic fermentation data, while our fermentation process was conducted under aerobic condition. Moreover, the strain species used in their work was also different from ours. Therefore it is necessary to develop a kinetic model to describe the fermentative production of 1,3-PD under aerobic condition, which can serve as a tool for further controlling and optimizing the fermentation process. In the present work we developed a macro-kinetic model with consideration of multiple products inhibitions to describe the cell growth, products formations, and substrate consumption during 1,3-PD production by *K. pneumoniae* HR526 under aerobic condition with glycerol as carbon source. The model was further applied to predict the cell growth and 1,3-PD concentration in batch, fed-batch, and continuous fermentations.

Materials and Methods

Microorganism and Fermentation Process

The bacterium used in the experiments was *K. pneumoniae* HR526, which was isolated and preserved in our laboratory. After activated at 30 °C for 12 h, the strain was transferred to a 250-mL flask containing 100 mL seeding medium followed by incubation at 30 °C and 140 rpm in an air-bath shaker (SKY-211B, SUKUN, China) for 12 h. The seeding medium consisted of 30 $g\cdot L^{-1}$ glycerol, 2 $g\cdot L^{-1}$ $(NH_4)_2SO_4$, 3.4 $g\cdot L^{-1}$ $K_2HPO_4\cdot 3H_2O$, 1.3 $g\cdot L^{-1}$ KH_2PO_4, 0.2 $g\cdot L^{-1}$ $MgSO_4\cdot 7H_2O$, 1 $g\cdot L^{-1}$ yeast extract, 2 $mL\cdot L^{-1}$ trace element solution, and 1.65 $mg\cdot L^{-1}$ Fe^{2+}. For batch fermentation, after the fermentation broth was inoculated with 1 % (*v/v*) inocula, the fermentation experiments were carried out in a 5-L stirred tank bioreactor (BIOSTAT B Plus, Sartorius, Germany) containing 4 L fermentation medium. The fermentation process was controlled at 37 °C, pH 6.5, 250 rpm, and 0.5 vvm air ventilation. The pH value was controlled by automatic addition of 30 % (wt) NaOH. The fermentation medium consisted of 25 $g\cdot L^{-1}$ glycerol, 4 $g\cdot L^{-1}$ $(NH_4)_2SO_4$, 0.69 $g\cdot L^{-1}$ $K_2HPO_4\cdot 3H_2O$, 0.25 $g\cdot L^{-1}$ KH_2PO_4, 0.2 $g\cdot L^{-1}$ $MgSO_4\cdot 7H_2O$, 1.5 $g\cdot L^{-1}$ yeast extract, 1 $mL\cdot L^{-1}$ trace element solution (containing 100 $g\cdot L^{-1}$ $MnSO_4\cdot 4H_2O$, 70 $g\cdot L^{-1}$ $ZnCl_2$, 35 $g\cdot L^{-1}$ $Na_2MoO_4\cdot 2H_2O$, 60 $g\cdot L^{-1}$ H_3BO_3, 200 $g\cdot L^{-1}$ $CoCl_2\cdot 6H_2O$, 29.28 $g\cdot L^{-1}$ $CuSO_4\cdot 5H_2O$, 25 $g\cdot L^{-1}$ $NiCl_2\cdot 6H_2O$, and 0.9 $mL\cdot L^{-1}$ HCl (37 %), and 1.65 $mg\cdot L^{-1}$ Fe^{2+}. Samples were taken at regular intervals to measure the biomass, substrate, and products concentrations. For fed-batch fermentation, the start-up of the process was the same as that

of batch fermentation. When glycerol concentration was below 5 g·L^{-1}, glycerol was fed continuously to keep the glycerol concentration in the fermenter at 5–20 g·L^{-1}. The procedure of continuous fermentation was similar to that of fed-batch process, but equivalent fermentation broth was also continuously pumped out of the fermenter. The flow rate of feed stream was adjusted to obtain a desired dilution rate.

Analytical Methods

Biomass concentration was determined by measuring optical density (OD) at 650 nm with a spectrophotometer (SP-722E, Spectrum Shanghai, China). Dry cell weight was calculated according to OD data by a calibration curve obtained previously. The organic components were analyzed by high-performance liquid chromatography (HPLC, SHIMADZU, Japan) equipped with an Aminex HPX-87H column at 65 °C with 0.005 mol·L^{-1} H$_2$SO$_4$ as mobile phase at a flow rate of 0.8 mL min^{-1}. A RID-10A differential refractive index detector was used with an injection volume of 20 μL.

Data Processing Methods

The kinetic parameters were regressed according to experimental data by the least square method using Matlab 6.5 software to minimize the objective function ($f_{objective}$), which was the quadratic sum of the difference between calculated data ($f(x_i)$) and experimental data (y_i), as shown in the following expression:

$$f_{objective} = \sum_{i=1}^{n} \delta_i^2 = \sum_{i=1}^{n} [f(x_i) - y_i]^2 \qquad (1)$$

4-order Runge–Kutta method was used for the numerical solution of differential equations.

Results and Discussion

Analysis of Product Inhibitions on Cell Growth

When glycerol is used as a carbon source, one part of the substrate is consumed for cell biomass accumulation, and the other is used for supporting the bacterial metabolism. According to the metabolic network of glycerol in *K. pneumoniae* HR526, by-products such as acetic acid, succinic acid, and 2, 3-butanediol (2,3-BD) are formed in the oxidation pathway with generation of NADH and ATP, while in the reduction pathway, 1,3-PD is produced in the presence of NADH [25]. Previous studies have shown that multiple products inhibitions on the growth of *K. pneumoniae* existed clearly in 1,3-PD fermentation [26]. During fermentation the substrate glycerol, the main product 1,3-PD, and by-products 2,3-BD, acetate, and succinate may show inhibitions to cell growth. Therefore, the inhibitions of these components were investigated before developing kinetic models. The individual inhibitions of the products were studied by singly adding the compounds into the fermentation medium. In a fed-batch fermentation process, it was found that the intermediate product 3-hydroxypropionaldehyde (3-HPA) is toxic to cells [27–29]. If the initial glycerol concentration was higher than 30 g·L^{-1}, 3-HPA would accumulate to a high level which could cause cell death. Therefore, in the actual fermentation process, glycerol was fed continuously to carefully control its concentration. According to experimental data (data

not shown), when the initial glycerol concentration was lower than 30 g·L^{-1}, it exerted little inhibition. Therefore the inhibition of substrate glycerol on cell growth could be neglected, and our work was mainly focused on the product inhibitions. Figure 1 shows the experimental results of cell growth with different possible inhibitors present at different initial concentrations.

It can be known that 1,3-PD showed a significant inhibition to cell growth. After fermentation for 6 h, compared with those of the control experiments, biomass concentrations were reduced by 57.14, 62.34, 78.88, and 82.41 %, respectively, when initial 1,3-PD concentrations were 25, 50, 75, and 100 g·L^{-1}. The inhibition of byproduct 2,3-BD also could be clearly observed. After fermentation for 6 h, cell biomass concentrations were reduced by 43.01, 55.84, 73.01, and 77.35 %, respectively, when the initial 2,3-BD concentration was 20, 30, 40, and 50 g·L^{-1}. Similarly, the inhibition of acetate was also significant. Biomass concentrations were decreased by 70.85, 75.05, 81.15, and 84.62 % respectively with the initial acetate concentrations of 5, 10, 15, and 20 g·L^{-1}. Comparatively, by-product succinate showed much weaker inhibition. After fermentation for 6 h, with the initial succinate concentrations of 5–20 g·L^{-1}, biomass concentration was only reduced by less than 10 %. However, during fermentation, these products were co-present in the broth. The synergism effects of these products might show stronger inhibition. According to actual
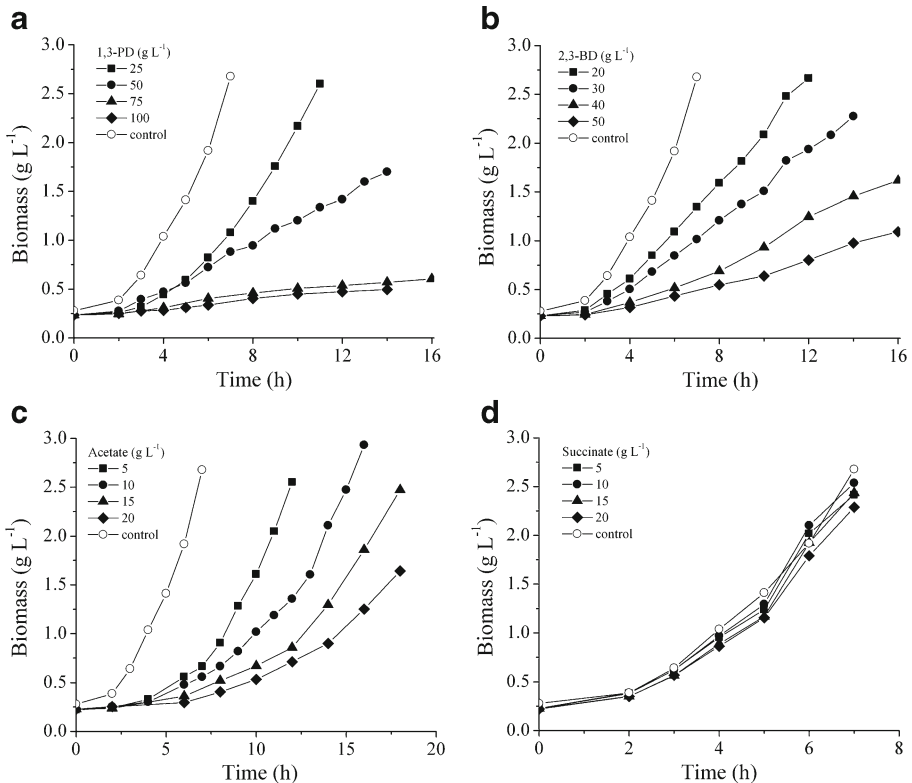

Fig. 1 Time courses of cell biomass concentration in batch fermentations with different possible inhibitors of several initial concentrations **a** 1,3-PD; **b** 2,3-BD; **c** acetate; **d** succinate; the initial glycerol concentration was 25 g·L^{-1}

fermentation process, at the end of exponential phase of K. pneumoniae HR526, the concentrations of 1,3-PD, 2,3-BD, acetate, and succinate were about 50, 12, 7, and 4 g·L^{-1}, respectively. Therefore, an orthogonal experiment design (Table 1) was conducted to investigate the inhibition of the multiple products when they were co-present in the fermentation broth. Biomass concentrations of the orthogonal experiments after fermentation for 6 h are shown in Table 1. It is clear that when the products were co-present in the fermentation broth, much stronger inhibition was observed. For instance, when the inhibitor concentrations were 45 g·L^{-1} of 1,3-PD, 16 g·L^{-1} of 2,3-BD, and 9 g·L^{-1} of acetate, after fermentation for 6 h, biomass concentration was reduced by 84.31 % (Run 8); however, when 1,3-PD, 2,3-BD, and acetate were solely added into the medium with initial concentrations of 50, 20, and 10 g·L^{-1}, biomass concentration was reduced by 62.34, 43.01, and 75.05 %, respectively. Statistic analysis of the data listed in Table 1 demonstrated that 1,3-PD, 2,3-BD, and acetate had very significant inhibitions to cell growth ($P<0.01$), while the inhibitive effect of succinate was insignificant ($P>0.1$). Therefore, investigating the kinetic modeling of 1,3-PD production with consideration of the inhibitive effects of these products can be helpful for further optimizing the fermentation process.

Development of Kinetic Model

A preliminary kinetic model was proposed to describe the fermentation performance, including cell growth, products formations, and substrate consumption. The cell growth rate of K. pneumoniae HR526 is described by Monod's equation, which indicates that the cell growth rate is the function of biomass concentration and single growth-limiting substrate (glycerol) concentration:

$$\frac{dX}{dt} = \mu_m \frac{S}{K_S + S} X \qquad (2)$$

where X is cell biomass concentration (g·L^{-1}); S is glycerol concentration (g·L^{-1}); μ_m is Monod maximum specific growth rate (h^{-1}); K_S is saturation constant (g·L^{-1}). According to aforementioned experimental results, the inhibition of succinate can be neglected. Therefore,

Table 1 Orthogonal experiments of multiple products inhibitions to cell growth (initial glycerol concentration 25 gL^{-1})

Run	Initial 1,3-PD concentration (g·L^{-1})	Initial 2,3-BD concentration (g·L^{-1})	Initial acetate concentration (g·L^{-1})	Initial succinate concentration (g·L^{-1})	Biomass concentration after 6 h (g·L^{-1})
Control	0	0	0	0	1.92
1	15	8	3	4	0.86
2	15	16	6	8	0.54
3	15	24	9	12	0.41
4	30	8	9	8	0.48
5	30	16	3	12	0.64
6	30	24	6	4	0.31
7	45	8	6	12	0.51
8	45	16	9	4	0.30
9	45	24	3	8	0.37

a linear model considering the inhibitions of 1,3-PD, 2,3-BD, and acetate is proposed as follows:

$$\mu_m = \mu'_m - k_1 \frac{P}{C_P^*} - k_2 \frac{P_B}{C_B^*} - k_3 \frac{P_A}{C_A^*} \qquad (3)$$

where μ'_m is maximum specific growth rate (h^{-1}), C_P^*, C_B^*, and C_A^* are critical inhibition concentrations of 1,3-PD, 2,3-BD, and acetate, respectively ($g \cdot L^{-1}$), and k_1, k_2, and k_3 are corresponding inhibition constants. The increase rate of biomass concentration during fermentation thus can be expressed as:

$$\frac{dX}{dt} = \left[\mu'_m - k_1 \frac{P}{C_P^*} - k_2 \frac{P_B}{C_B^*} - k_3 \frac{P_A}{C_A^*} \right] \frac{S}{K_S + S} X \qquad (4)$$

The formation rates of the main product 1,3-PD and by-products 2,3-BD, acetate, and succinate are described by the following equations, respectively, which indicate that the products formations are associated with cell growth rate and biomass concentration. It has been observed that after fermentation for a certain time, the products concentrations stopped increasing; therefore feedback inhibition items are introduced as shown in the following equations:

$$\frac{dP}{dt} = \alpha \frac{dX}{dt} + \beta X \left(1 - \frac{P}{P^*} \right) \qquad (5)$$

$$\frac{dP_B}{dt} = \alpha_B \frac{dX}{dt} + \beta_B X \left(1 - \frac{P_B}{P_B^*} \right) \qquad (6)$$

$$\frac{dP_A}{dt} = \alpha_A \frac{dX}{dt} + \beta_A X \left(1 - \frac{P_A}{P_A^*} \right) \qquad (7)$$

$$\frac{dP_S}{dt} = \alpha_S \frac{dX}{dt} + \beta_S X \left(1 - \frac{P_S}{P_S^*} \right) \qquad (8)$$

where P, P_B, P_A, and P_S are concentrations of 1,3-PD, 2,3-BD, acetate, and succinate, respectively (gL^{-1}); P^*, P_B^*, P_A^*, and P_S^* are critical feedback inhibition concentrations ($g \cdot L^{-1}$) of 1,3-PD, 2,3-BD, acetate, and succinate, respectively. The consumption rate of substrate glycerol thus can be described by the following equation, which indicates that substrate glycerol is used for cell growth, formation of all products, and maintaining the cellular metabolic activities:

$$-\frac{dS}{dt} = \frac{1}{Y_{X/S}} \frac{dX}{dt} + mX + \frac{1}{Y_{P/S}} \frac{dP}{dt} + \frac{1}{Y_{P_B/S}} \frac{dP_B}{dt} + \frac{1}{Y_{P_A/S}} \frac{dP_A}{dt} + \frac{1}{Y_{P_S/S}} \frac{dP_S}{dt} \qquad (9)$$

where $Y_{X/S}$, $Y_{P/S}$, $Y_{PB/S}$, $Y_{PA/S}$, and $Y_{PS/S}$ are yield coefficients for biomass, 1,3-PD, 2,3-BD, acetate, and succinate on glycerol, respectively ($g \cdot g^{-1}$); m is the kinetic constant for cellular metabolism (h^{-1}).

Determination of Kinetic Constants

The regressed parameters are shown in Table 2, which were determined by more than 20 groups of experimental data (data shown in Fig. 1 and Table 1). Corresponding determination coefficients for model regression were in the range of 0.83–0.98, and P values were lower than 0.01, indicating that the experimental data could be well described by the kinetic model. It can be known that 1,3-PD showed the highest critical inhibition concentrations (98.76 g·L^{-1}), but acetate had the highest inhibition constants (0.4974). It illustrated that the growth of $K.$ $pneumoniae$ HR526 were the most sensitive to acetate when the concentration of the product was at a certain value. For example, from Fig. 1 it can be known that cell growth was strongly inhibited at 20 g·L^{-1} acetate, but the strain still showed a relatively high growth rate when the initial concentrations of 1,3-PD and 2,3-BD were 25 and 20 g·L^{-1}, respectively. However, the inhibitive effects of the products was strongly dependent on their concentrations, and the concentrations of 1,3-PD and 2,3-BD were always much higher than that of acetate in an actual fermentation process. Therefore, 1,3-PD and 2,3-BD were more important than acetate to inhibit cell growth.

In the work of Xiu et al., they found that the maximum specific growth rate (μ_m), saturation constant (K_S), constant for cellular metabolism (m), yield coefficient (α), and constants β of 1,3-PD were 0.67 h^{-1}, 2.58×10^{-2} g·L^{-1} (0.28 mmol·L^{-1}), 0.202 h^{-1} (2.20 mmol·g^{-1}·h^{-1}), 5.14 g·g^{-1} (67.69 mmol·g^{-1}), and -0.204 h^{-1} (-2.69 mmol·g^{-1}·h^{-1}), respectively [24]. In the work of Cheng, the maximum specific growth rate (μ_m), the yield coefficient (α), and constants β of 1,3-PD, constant for cellular metabolism (m), yield coefficients of biomass ($Y_{X/S}$), and 1,3-PD ($Y_{P/S}$) were 0.2 h^{-1}, 8.55 g·g^{-1}, 0.68 h^{-1}, 0.15 h^{-1}, 0.05 g·g^{-1}, and 0.56 g·g^{-1}, respectively [30]. In our work, the maximum specific growth rate ($\mu_m^{'}$), saturation constant (K_S), the yield coefficient (α) and constants β of 1,3-PD, constant for cellular metabolism (m), the yield coefficients of biomass ($Y_{X/S}$), and 1,3-PD ($Y_{P/S}$) were determined to be 0.42 h^{-1}, 2.18 g·L^{-1}, 4.74 g·g^{-1} and 0.91 h^{-1}, 0.46 h^{-1}, 0.68 g·g^{-1}, and 1.48 g·g^{-1}, respectively. Some of the parameters were similar, but some were significantly different. However, since the kinetic constants are strongly dependent on the strain species and fermentation conditions, further comparison should be supported by more

Table 2 Regressed values of parameters of the kinetic model

Parameter	Unit	Value	Parameter	Unit	Value
$\mu_m^{'}$	h^{-1}	0.4162	m	h^{-1}	0.4626
k_1	h^{-1}	0.3550	α	g·g^{-1}	4.7413
k_2	h^{-1}	0.2764	α_B	g·g^{-1}	0.6467
k_3	h^{-1}	0.4974	α_A	g·g^{-1}	0.8711
C_P^*	g·L^{-1}	98.76	α_S	g·g^{-1}	0.3076
C_B^*	g·L^{-1}	58.74	β	h^{-1}	0.9131
C_A^*	g·L^{-1}	36.62	β_B	h^{-1}	0.3322
K_S	g·L^{-1}	2.1827	β_A	h^{-1}	0.1386
$Y_{X/S}$	g·g^{-1}	0.6838	β_S	h^{-1}	0.1402
$Y_{P/S}$	g·g^{-1}	1.4808	P^*	g·L^{-1}	98.40
$Y_{P_B/S}$	g·g^{-1}	0.5531	P_B^*	g·L^{-1}	40.15
$Y_{P_A/S}$	g·g^{-1}	4.3587	P_A^*	g·L^{-1}	7.68
$Y_{P_S/S}$	g·g^{-1}	0.4437	P_S^*	g·L^{-1}	13.09

comprehensive experimental data. Anyway, the experimental data showed that *K. pneumoniae* HR526 had a good ability to produce 1,3-PD.

Applications of the Kinetic Model

The objective of kinetic study is to develop a model for describing the consumption of substrate and formations of products, and whereby the model can be further applied to predict the data under various fermentation conditions. Therefore, we further used the developed model to predict glycerol consumption and products formations in different fermentation processes.

Batch Fermentation

Batch fermentation experiments were conducted with initial glycerol concentrations of 20 and 30 g·L^{-1}, respectively. The experimental and model-calculated results on cell growth, products formations, and substrate consumption are shown in Fig. 2. After fermentation for 4 h (timing started at the beginning of exponential phase) with 20 g·L^{-1} initial glycerol, the concentrations of cell biomass, glycerol, 1,3-PD, 2,3-BD, acetate, and succinate were 2.45, 2.63, 10.36, 2.87, 2.11, and 1.18 g·L^{-1}, respectively, and corresponding model-calculated concentrations were 1.91, 0.14, 10.82, 2.73, 1.99, and 1.16 g·L^{-1}. When initial glycerol concentration was increased to 30 gL^{-1}, after fermentation for 5 h the concentrations of cell biomass, glycerol, 1,3-PD, 2,3-BD, acetate, and succinate were 2.68, 4.44, 13.53, 3.10, 2.83, and 1.39 g·L^{-1}, respectively, and corresponding model-calculated concentrations were 2.71, 0.38, 16.83, 4.11, 2.94, and 1.77 g·L^{-1}. It indicated that the model generally could well predict the experimental data, and could be applied for predicting the kinetic behavior of batch fermentation process.

Fed-Batch Fermentation

As aforementioned description, in order to avoid the accumulation of intermediate product 3-HPA, fed-batch fermentation are usually employed for fermentative production of 1,3-PD to control glycerol concentration at a relatively low level (usually less than 20 gL^{-1}).
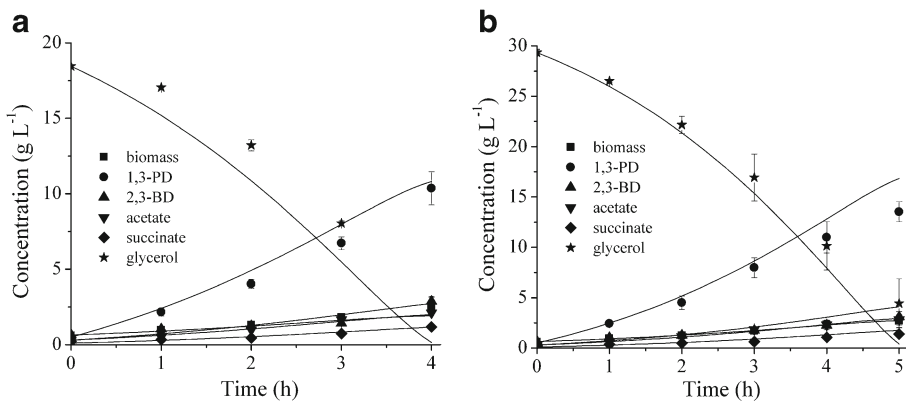

Fig. 2 Experimental (*symbols*) and calculated results (*solid lines*) of biomass, products, and substrate concentrations in batch fermentations with different initial glycerol concentrations **a** 20 g·L^{-1}; **b** 30 g·L^{-1}

Therefore, in an actual fed-batch fermentation, the feed rate of glycerol usually does not keep at a constant. During fed-batch fermentation, the volume of fermentation broth gradually increases, thus the kinetic model should be revised as follows:

$$\frac{d(VX)}{dt} = \mu XV \tag{10}$$

$$\frac{d(VP)}{dt} = \alpha\frac{d(VX)}{dt} + \beta X\left(1 - \frac{P}{P^*}\right)V \tag{11}$$

$$\frac{d(VP_B)}{dt} = \alpha_B\frac{d(VX)}{dt} + \beta_B X\left(1 - \frac{P_B}{P_B^*}\right)V \tag{12}$$

$$\frac{d(VP_A)}{dt} = \alpha_A\frac{d(VX)}{dt} + \beta_A X\left(1 - \frac{P_A}{P_A^*}\right)V \tag{13}$$

$$\frac{d(VP_S)}{dt} = \alpha_S\frac{d(VX)}{dt} + \beta_S X\left(1 - \frac{P_S}{P_S^*}\right)V \tag{14}$$

$$-\frac{d(VS)}{dt} = \frac{1}{Y_{X/S}}\frac{d(VX)}{dt} + mXV + \frac{1}{Y_{P/S}}\frac{d(VP)}{dt} + \frac{1}{Y_{P_B/S}}\frac{d(VP_B)}{dt} + \frac{1}{Y_{P_A/S}}\frac{d(VP_A)}{dt}$$
$$+ \frac{1}{Y_{P_S/S}}\frac{d(VP_S)}{dt} - FS_0 \tag{15}$$

$$\frac{dV}{dt} = F \tag{16}$$

where V is the volume of fermentation broth (L), F is the feed rate of glycerol (L·h^{-1}) and S_0 is the concentration of feed glycerol (g·L^{-1}). A 48-h fed-batch fermentation experiment was conducted and the experimental results were compared with model-calculated data. The initial glycerol concentration was 20 g·L^{-1} and glycerol was fed at the third hour. The experimental and model-calculated results are shown in Fig. 3. It can be known that a relatively accurate result can be observed between experimental and calculated results. Particularly, the model could well predict the biomass, 1,3-PD, 2,3-BD, acetate, and succinate concentrations. However, there were high deviations for glycerol concentration. According to experimental results, after fermentation for 48 h, the concentrations of cell biomass, glycerol, 1,3-PD, 2,3-BD, acetate, and succinate were 6.51, 31.96. 93.40, 28.93, 7.06, and 13.49 g·L^{-1}, respectively, and corresponding model-calculated concentrations were 5.72, 23.77, 87.23, 33.57, 7.50, and 12.45 g·L^{-1}, respectively. It illustrated that the model generally could be applied for predicting 1,3-PD concentration in fed-batch fermentation.

Fig. 3 Experimental (*symbols*) and calculated results (*solid lines*) of biomass, products, and substrate concentrations in fed-batch fermentation
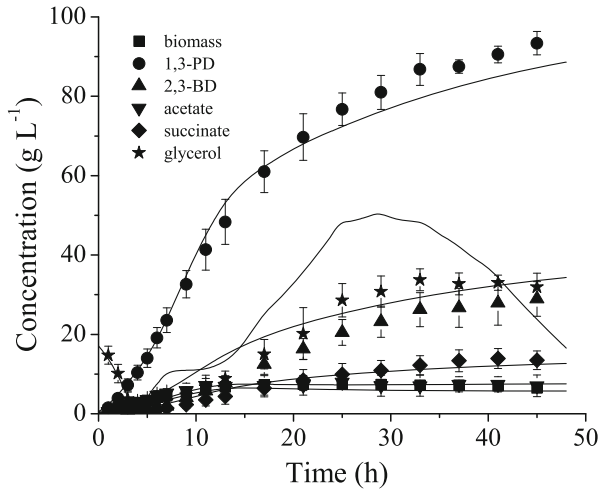
Continuous Fermentation

To further verify the accuracy of the kinetic model, a continuous fermentation was conducted with initial glycerol concentration of 20 g·L^{-1}. Before the feed stream was continuously fed into fermenter, a batch process was performed for 12 h to increase cell biomass. Subsequently, continuous fermentation started at a dilution rate of 0.12 h^{-1}. The glycerol concentration of the feed stream was 70 g·L^{-1}. The experimental results for biomass, products, and substrate concentrations are shown in Fig. 4.

When the fermentation process reaches the steady-state, the kinetic model can be expressed as follows:

$$\frac{dX}{dt} = \mu X - DX = 0 \tag{17}$$

Fig. 4 Experimental results of biomass, products, and substrate concentrations in a continuous fermentation
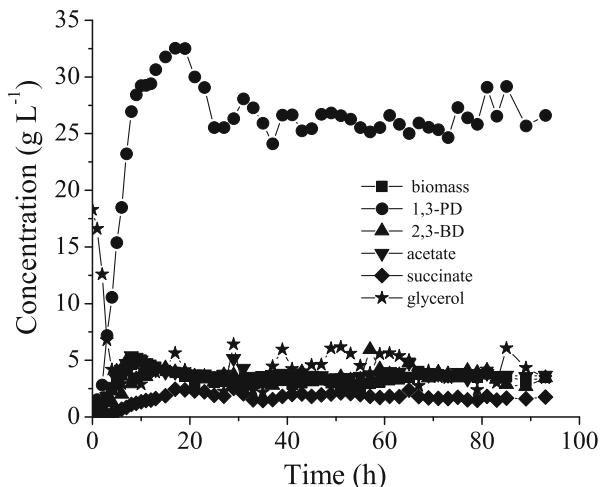
Table 3 Experimental and calculated results of continuous fermentation

	Experimental	Calculated
Biomass concentration (g·L^{-1})	3.38±0.64	3.30
Glycerol concentration (g·L^{-1})	4.30±2.12	4.42
1,3-PD concentration (g·L^{-1})	26.63±2.53	32.47
2,3-BD concentration (g·L^{-1})	3.72±1.04	9.18
Acetate concentration (g·L^{-1})	4.25±0.91	4.47
Succinate concentration (g·L^{-1})	1.99±0.53	3.76
1,3-PD productivity (g·L^{-1}·h^{-1})	3.22±1.95	3.90
1,3-PD yield on glycerol (g·g^{-1})	0.44±0.03	0.50

$$\frac{dP}{dt} = \alpha \frac{dX}{dt}_G + \beta X \left(1 - \frac{P}{P^*}\right) - DP = 0 \tag{18}$$

$$\frac{dP_B}{dt} = \alpha_B \frac{dX}{dt}_G + \beta_B X \left(1 - \frac{P_B}{P_B^*}\right) - DP_B = 0 \tag{19}$$

$$\frac{dP_A}{dt} = \alpha_A \frac{dX}{dt}_G + \beta_A X \left(1 - \frac{P_A}{P_A^*}\right) - DP_A = 0 \tag{20}$$

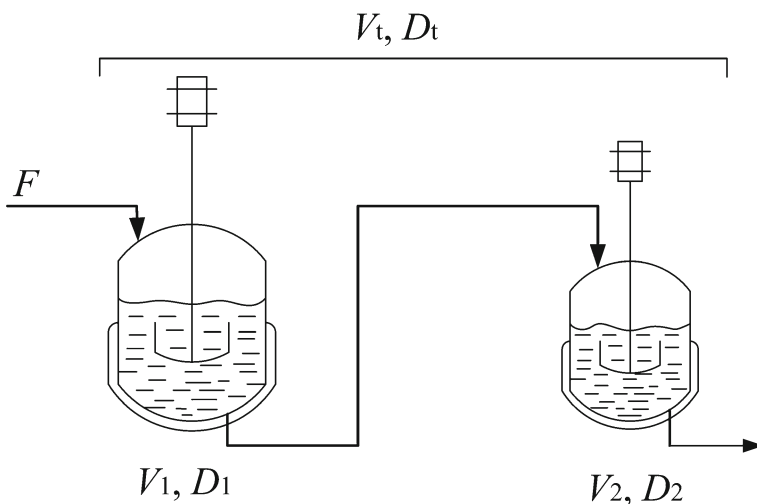$$\frac{dP_S}{dt} = \alpha_S \frac{dX}{dt}_G + \beta_S X \left(1 - \frac{P_S}{P_S^*}\right) - DP_S = 0 \tag{21}$$

Fig. 5 Scheme for two-stage process for fermentative production of 1,3-propanediol

Table 4 Calculated optimal dilution rate of each stage at several total dilution rates for a two-stage fermentation process

Total dilution rate, D_t (h^{-1})	Dilution rate of the first stage, D_1 (h^{-1})	Dilution rate of the second stage, D_2 (h^{-1})
0.021	0.044	0.40
0.028	0.060	0.052
0.042	0.090	0.078

$$-\frac{dS}{dt} = \left(\frac{1}{Y_{X/S}}\frac{dX}{dt}_G + mX + \frac{1}{Y_{P/S}}\frac{dP}{dt}_G + \frac{1}{Y_{P_B/S}}\frac{dP_B}{dt}_G + \frac{1}{Y_{P_A/S}}\frac{dP_A}{dt}_G + \frac{1}{Y_{P_S/S}}\frac{dP_S}{dt}_G \right) \quad (22)$$
$$-D(S_0 - S) = 0$$

where D is dilution rate (h^{-1}) and S_0 is glycerol concentration of feed stream (g·L^{-1}). The experimental results and model-calculated results are summarized in Table 3. It can be known that the model-calculated data were somewhat larger than the experimental data of products, while the predicted substrate concentrations were lower than those of experimental results. These deviations were mainly because that the kinetic constants were regressed by batch fermentation data which naturally showed some difference to the fermentation behavior of continuous fermentation. However, the experimental results showed that the model generally could be applied for predicting continuous fermentation process with satisfactory accuracy.

The developed kinetic model can be as a tool to further optimize the continuous fermentation process. For example, for a two-stage fermentation process as shown in Fig. 5, at a fixed total fermentation volume V_t (or total dilution rate, D_t), the fermentation volume ratio (or dilution rate ratio) of the first and second stages (V_1/V_2) (or D_1/D_2) can affect the residence time respectively and thus affecting the product concentration in

Table 5 Experimental and model-calculated data for 1,3-PD concentration, productivity, and yield in a two-stage continuous process

D_t (h^{-1})	D_1 (h^{-1})	D_2 (h^{-1})	Experimental data				Model-calculated data			
			C_{P1} (g·L^{-1})	C_{P2} (g·L^{-1})	P_{ro} (g·L^{-1}·h^{-1})	Y_P (g·g^{-1})	C_{P1} (g·L^{-1})	C_{P2} (g·L^{-1})	P_{ro} (g·L^{-1}h^{-1})	Y_P (g·g^{-1})
0.042	0.09[a]	0.078[a]	34.31	61.23	2.55	0.40	32.15	57.68	2.41	0.38
0.042	0.12	0.064	28.22	58.21	2.43	0.43	28.11	56.13	2.34	0.41
0.042	0.15	0.058	21.98	53.13	2.21	0.43	22.01	50.16	2.09	0.40
0.028	0.06[a]	0.052[a]	42.31	68.11	1.89	0.47	39.12	65.69	1.83	0.46
0.028	0.08	0.043	33.34	67.28	1.87	0.43	32.16	63.21	1.76	0.41
0.028	0.12	0.036	28.22	63.04	1.75	0.40	26.17	61.22	1.70	0.39
0.021	0.044[a]	0.040[a]	38.08	70.26	1.46	0.37	40.52	77.10	1.62	0.40
0.021	0.06	0.032	40.78	73.31	1.53	0.40	42.98	73.52	1.53	0.40
0.021	0.1	0.026	32.09	69.90	1.46	0.37	35.26	68.12	1.42	0.36

D_1 dilution rate of the first stage, D_2 dilution rate of the second stage, C_{P1} 1,3-PD concentration in the first-stage fermenter, C_{P2} 1,3-PD concentration in the second-stage fermenter, P_{ro} the total productivity of 1,3-PD, Y_P yield of 1,3-PD based on glycerol

[a] The calculated optimal dilution rates according to kinetic model

effluent. According to the kinetic model, the optimal dilution rates of each stage at several fixed total dilution rates can be calculated as shown in Table 4. Experimental results further verified that there was indeed an optimal dilution rate for each stage to obtain the highest 1,3-PD concentration and productivities as shown in Table 5, and the optimal dilution rates for each stage determined by kinetic model were generally in accordance with those determined by experiments. The results also showed that in two-stage fermentation, decreasing total dilution rate (increasing total residence time) could increase final 1,3-PD concentration but decrease productivity. Therefore, a compromise should be made. According to Table 5, the total dilution rate of $0.028\ \mathrm{h^{-1}}$ (total residence time of 36 h) was satisfied for two-stage fermentation, and the optimal D_1 and D_2 were 0.06 and $0.052\ \mathrm{h^{-1}}$, respectively. The experimental results demonstrated that the kinetic model was reliable as a tool to optimize the process parameters for fermentative production of 1,3-PD.

Conclusions

The inhibitive effects of several products on cell growth of *K. pneumoniae* HR526 for 1,3-propanediol (1,3-PD) production under aerobic condition were investigated with glycerol as carbon source. It was found that during the fermentative production of 1,3-PD, to accurately describe the kinetics of the fermentation process the multiple product inhibitions cannot be negligible. A kinetic model with consideration of multiple product inhibitions thus was proposed to describe the fermentative production of 1,3-PD. Corresponding kinetic constants were regressed according to the experimental data of batch fermentation. It was found that 1,3-PD, 2,3-BD, and acetate showed strong inhibition to cell growth depending on their concentrations. Comparison of experimental results of batch, fed-batch, and continuous fermentations indicated that the kinetic model was relatively accurate to predict experimental data. The model thus can serve as a tool for further controlling and optimizing the fermentation process.

References

1. Huang, H., Gong, C. C., & Tsao, G. T. (2002). Production of 1, 3-propanediol by *Klebsiella pneumoniae*. *Applied Biochemistry and Biotechnology, 98*, 687–698.
2. Zeng, A. P., & Biebl, H. (2002). Bulk chemicals from biotechnology: the case of 1, 3-propanediol production and the new trends. *Advances in Biochemical Engineering/Biotechnology, 74*, 239–259.
3. Biebl, H., Menzel, K., Zeng, A. P., & Deckwer, W. D. (1999). Microbial production of 1, 3-propanediol. *Applied Microbiology and Biotechnology, 52*, 289–297.
4. Arntz, D., Haas, T., Müller, A., & Wiegand, N. (1991). Kinetische untersuchung zur hydrat isierung von acrolein. *Chem. Ing. Tech., 63*, 733–735.
5. Besson, M., Gallezot, P., Pigamo, A., & Reifsnyder, S. (2003). Development of an improved continuous hydrogenation process for the production of 1, 3-propanediol using titania supported ruthenium catalysts. *Appl. Catal. A, 250*, 117–124.
6. Knifton, J. F., James, T. G., Slaugh, L. H., Allen, K. D., Weider, P. R. and Powell J. B. (2004). One-step production of 1, 3-propanediol from ethylene oxide and syngas with a cobalt-iron catalyst. US Patent 6.750.373.
7. Biebl, H., & Marten, S. (1995). Fermentation of glycerol to 1, 3-propanediol: use of cosubstrates. *Applied Microbiology and Biotechnology, 44*, 15–19.
8. Decker, W. D. (1995). Microbial conversion of glycerol to 1, 3-propanediol, in International Congress on Beyond 2000—Chemicals from Biotechnology: Ecological Challenge and Economic Restraints, Proc. *FEMS Microbiology Reviews, 16*, 143–149.

9. Xu, Y. Z., Liu, H. J., Du, W., Sun, Y., Ou, X. J., & Liu, D. H. (2009). Integrated production for biodiesel and 1, 3-propanediol with lipase-catalyzed transesterification and fermentation. *Biotechnol. Let., 31*, 1335–1341.

10. Charles, E. N., & Gregory, M. W. (2003). Metabolic engineering for the microbial production of 1, 3-propanediol. *Current Opinion in Biotechnology, 14*, 454–459.

11. Zheng, Z. M., Xu, Y. Z., Liu, H. J., Guo, N. N., Cai, Z. Z., & Liu, D. H. (2008). Physiologic mechanisms of sequential products synthesis in 1, 3-propanediol fed-batch fermentation by *Klebsiella pneumoniae. Biotechnology and Bioengineering, 100*, 923–932.

12. Chen, Z., Liu, H. J., Zhang, J. A., & Liu, D. H. (2009). Cell physiology and metabolic flux response of *Klebsiella pneumoniae* to aerobic conditions. *Process Biochemistry, 44*, 862–868.

13. Xu, Y. Z., Guo, N. N., Zheng, Z. M., Ou, X. J., Liu, H. J., & Liu, D. H. (2009). Metabolism in 1, 3-propanediol fed-batch fermentation by a D-lactate deficient mutant of *Klebsiella pneumoniae. Biotechnology and Bioengineering, 104*, 965–972.

14. Chen, Z., Liu, H. J., & Liu, D. H. (2011). Metabolic pathway analysis of 1, 3-propanediol production with a genetically modified *Klebsiella pneumoniae* by overexpressing an endogenous NADPH-dependent alcohol dehydrogenase. *Biochemical Engineering Journal, 54*, 151–157.

15. Cheng, K. K., Liu, D. H., Sun, Y., & Liu, W. B. (2004). 1, 3-Propanediol production by *Klebsiella pneumoniae* under different aeration strategies. *Biotechnology Letters, 26*, 911–915.

16. Zheng, Z. M., Hu, Q. L., Hao, J., Xu, F., Guo, N. N., Sun, Y., et al. (2008). Statistical optimization of culture conditions for 1, 3-propanediol by *Klebsiella pneumoniae* AC 15 via central composite design. *Bioresource Technology, 99*, 1052–1056.

17. Zheng, Z. M., Guo, N. N., Hao, J., Cheng, K. K., Sun, Y., & Liu, D. H. (2009). Scale-up of micro-aerobic 1, 3-propanediol production with *Klebsiella pneumonia* CGMCC 1.6366. *Process Biochemistry, 44*, 944–948.

18. Zheng, Z. M., Xu, Y. Z., Wang, T. P., Dong, C. Q., Yang, Y. P., & Liu, D. H. (2010). Ammonium and phosphate limitation in 1, 3-propanediol production by *Klebsiella pneumoniae. Biotechnology Letters, 32*, 289–294.

19. Zeng, A. P., Ross, A., Biebl, H., Tag, C., Günzel, B., & Deckwer, W. D. (1994). Multiple product inhibition and growth modeling of *Clostridium butyricum* and *Klebsiella pneumoniae* in glycerol fermentation. *Biotechnology and Bioengineering, 44*, 902–911.

20. Zeng, A. P. (1995). A kinetic model for product formation of microbial and mammalian cells. *Biotechnology and Bioengineering, 46*, 314–324.

21. Zeng, A. P., & Deckwer, W. D. (1995). A kinetic model for substrate and energy consumption of microbial growth under substrate-sufficient conditions. *Biotechnol. Progr., 11*, 71–79.

22. Chen, Z., Zheng, Z. M., Sun, Y., Hong, A. A., Peng, F., Liu, C. M., et al. (2009). Fermentation characteristics of the fast conversion of glycerol to 1, 3-propanediol by *Klebsiella pneumoniae* HR526. *Microbiology, 36*, 799–803.

23. Liu, H. J., Xu, Y. Z., Zheng, Z. M., & Liu, D. H. (2010). 1, 3-Propanediol and its copolymers: research, development and industrialization. *Biotechnology Journal, 5*, 1137–1148.

24. Xiu, Z. L., Zeng, A. P., & An, L. J. (2000). Mathematical modeling of kinetics and research on multiplicity of glycerol bioconversion to 1, 3-propanediol. *J Dalian Univ Technol, 40*, 428–433.

25. Hao, J., Lin, R. H., Zheng, Z. M., Liu, H. J., & Liu, D. H. (2008). Isolation and characterization of microorganisms able to produce 1, 3-propanediol under aerobic conditions. *World Journal of Microbiology and Biotechnology, 24*, 1731–1740.

26. Cheng, K. K., Liu, H. J., & Liu, D. H. (2005). Multiple growth inhibition of *Klebsiella pneumoniae* in 1, 3-propanediol fermentation. *Biotechnology Letters, 27*, 19–22.

27. Zheng, Z. M., Cheng, K. K., Hu, Q. L., Liu, H. J., Guo, N. N., & Liu, D. H. (2008). Effect of culture conditions on 3-hydroxypropionaldehyde detoxification in 1, 3-propanediol fermentation by *Klebsiella pneumoniae. Biochemical Engineering Journal, 39*, 305–310.

28. Hao, J., Lin, R. H., Zheng, Z. M., Sun, Y., & Liu, D. H. (2008). 3-Hydroxypropionaldehyde guided glycerol feeding strategy in aerobic 1, 3-propanediol production by *Klebsiella pneumoniae. Journal of Industrial Microbiology and Biotechnology, 35*, 1615–1624.

29. Chen, Z., Liu, H. J., & Liu, D. H. (2009). Regulation of 3-hydroxypropionaldehyde accumulation in *Klebsiella pneumoniae* by overexpression of dhaT and dhaD genes. *Enzyme and Microbial Technology, 45*, 305–309.

30. Cheng, K. K., Lin, R. H., Liu, H. J., & Liu, D. H. (2005). Kinetic analysis of anaerobic fermentation of 1, 3-propanediol by *Klebsiella pneumoniae. The Chinese Journal of Process Engineering, 5*, 425–429.